crystals

MDPI

Supplementary Materials

S1. Synthesis of HZSM zeolites, NA/HZSM and NA:M/HZSM nanocomposites

Table S1. Synthesis conditions for the studied zeolites HZSM (Si/Al) and ZSM (Si/Ti) (TS) [16, 33, 34].

Zeolite	Si/*T*[1]/ Si/T[3]	Chemical composition[2], wt.%				Synthesis Description
		Al	Na	Fe	Ti	
MFI-Type Aluminosilicalites						
HZSM(12)	12/14	3.2	0.04	0.02	-	Zeolite International, USA
HZSM(25)	25/24	1.9	0.01	0.07	-	Template - n-butanol (analytical grade, Russia) – C_4H_9OH Silicon source: silica sol 30 wt. % (SiO_2, analytical grade, Russia) - silicic acid sol $nSiO_2 \cdot mH_2O$ Aluminum source: aluminum sulfate crystalline hydrate (analytical grade, Sigma-Aldrich) - $Al_2(SO_4)_3 \cdot 18H_2O$ Composition of aluminosilicate gel: 10 Na_2O-12 BuOH-Al_2O_3-50 SiO_2-1500 H_2O Synthesis conditions: holding the gel in the presence of NaZSM-5 seed crystals (5 wt% based on SiO_2 in the gel) in a 0.6 L autoclave under hydrothermal conditions for 50 hours at T = 438 K and vigorous stirring (90 rpm); separation of sediment by centrifugation; drying at T = 373-403 K; calcination at T ≥ 773 K; two ion exchanges in 1M ammonium nitrate solution (NH_4NO_3); drying and calcining the precipitate at T = 723-753 K for 2 hours
HZSM(40)	40/52	0.9	0.03	0.02	-	Template: $C_8H_{20}BrN$ (analytical grade, Sigma-Aldrich) Silicon source: silicic acid (analytical grade, Russia)– $nSiO_2 \cdot mH_2O$ Aluminum source: aluminum sulfate crystalline hydrate (analytical grade, Sigma-Aldrich) – $Al_2(SO_4)_3 \cdot 18H_2O$ Composition of aluminosilicate gel: 11 Na_2O-8 TEABr-Al_2O_3-80 SiO_2-1200 H_2O Synthesis conditions: exposure of the gel in hydrothermal conditions for 20 hours at T = 443 K; separation of sediment by centrifugation; drying at T = 373-403 K; calcination at T ≥ 773 K; two ion exchanges in ammoniacal buffer (54 g NH_4Cl + 50 mL 25% NH_4OH)/1 L buffer solution; calcination of the precipitate at T = 723-753 K for 2 hours

HZSM(300)	300/ 295-337	0.14-0.16	0.06	0.02	-	Template: $(CH_3)_4NOH$ (20% water solution Fluka, analytical grade, Sigma-Aldrich) Silicon source: silica sol 30 wt. % (SiO_2, analytical grade, Russia) - silicic acid sol $nSiO_2 \cdot mH_2O$ Aluminum source: sodium aluminate ($NaAlO_2$) solution (analytical grade, Sigma-Aldrich) Composition of aluminosilicate gel: $36Na_2O$-50TPAOH-Al_2O_3-600 SiO_2-3600 H_2O; Synthesis conditions: exposure of the gel in hydrothermal conditions for 40 hours at T = 443 K; separation of sediment by centrifugation; drying at T = 373-403 K; calcination at T ≥ 773 K; two ion exchanges in ammoniacal buffer (54 g NH_4Cl + 50 mL 25% NH_4OH)/1 L buffer solution; calcination of the precipitate at T = 723-753 K for 2 hours
MFI-Type Titanosilicalites						
TS-1 *TS-2* *TS-3*	-	-	-	-	-	Samples from different batches, *Zeolite International, USA, Product ZD 07031, Zeolite – CAS 1318-02-1* The TiO_2 content (3.1 wt. % TiO_2) in the sample was known only for TS-2 and TS-3.
TS-4	-	-	-	-	-	Template: tetrapropylammonium hydroxide $C_{12}H_{29}NO$ - TPAOH (40 wt. %., analytical grade, Sigma-Aldrich, CAS # 4499-86-9) Silicon source: tetraethylorthosilicate $Si(C_2H_5O)_4$ - TEOSi (22.5 g; analytical grade, TU 6-09-11-2153-94, Sibreaktiv JSC) Titanium source: tetraethyl orthotitanate $Ti(OC_2H_5)_4$ - TEOTi (analytical grade, TU 6-09-11-2170-97) Synthesis conditions: mixing of $Si(C_2H_5O)_4$ with 0.75 g TEOTi, keeping the mixture in a closed glass container for 1 h at room temperature. Addition the mixture dropwise to 62 ml of TPAOH aqueous solution placed in a closed container with a reflux condenser and a magnetic stirrer. Heating the mixture to 333 K, holding for 3 h with constant stirring. Transfer of the obtained sol to the autoclave, holding at 448 K under hydrothermal conditions for 72 h. Separation of the solid sediment by centrifugation, drying for 24 h at room temperature and 10 h at 383 K. Removal of the organic template (TPAOH) in a forced air muffle furnace at 823 K for 4-6 h.

[1] determined by the aluminosilicate gel composition

[2] determined by the chemical analysis method on the zeolites obtained without taking into account the presence of zeolite water

[3] recalculated according to the chemical analysis results

Nanocomposites with NA have been obtained by several methods:

Method 1a. Synthesis of NA/HZSM *in situ*: mixture of $TiOSO_4 \times xH_2SO_4 \times yH_2O$ (analytical grade, Sigma-Aldrich) (0.027 mol) and 40 mL distilled H_2O, heating to 363 K, carrying out hydrolysis for 3 min with vigorous stirring (magnetic stirrer, rotation speed 450-500 rpm), addition of zeolite (0.25 g) into the reaction mixture, hydrolysis at 366 K for 4 min., separation of the obtained solid phase by vacuum filtration, washing it with distilled water (20 ml, 3 times) and acetone (20 ml, 2 times), and drying at 363 K [66]. A modification of this method consists in reducing the reaction temperature (below the boiling point of water - 373.2 K) in an open system.

Method 1b. Synthesis of NA/HZSM-1 *in situ*: mixture of $TiOSO_4 \times xH_2O$ (analytical grade, Sigma-Aldrich) (0.026 mol) and 40 mL distilled H_2O, heating to 363 K, carrying out hydrolysis for 3 min with vigorous stirring (magnetic stirrer, rotation speed 450-500 rpm), addition of zeolite (0.3 g) into the reaction mixture, hydrolysis at 368 K for 4 min., separation of the obtained solid phase by vacuum filtration, washing it with distilled water (20 ml, 3 times) and acetone (20 ml, 2 times), and drying at 363 K [68].

Method 2. Synthesis of NA/HZSM-2 *in situ* by sol-gel method: mixture of $Ti(OC_4H_9)_4$ (analytical grade, Sigma-Aldrich) (0.012 mol), 40 mL n-butanol (C_4H_9OH) and 3 mL concentrated HNO_3 at 298 K, addition of zeolite (0.3 g) into the mixture, holding for 168 hours. Prepared gel was dried at 363 K. [68].

Method 3. Synthesis of NA/HZSM-3 *in situ* by introduction of doping elements (V^{5+} in the form of $VO(NO_3)_3$, Ni^{2+} in the form of $Ni(NO_3)_2 \times 6H_2O$ and Ag^+ in the form of $AgNO_3$ (analytical grade, Sigma-Aldrich)): mixture of $TiOSO_4 \times xH_2O$ (analytical grade, Sigma-Aldrich) (0.015 mol) and 40 mL distilled H_2O, heating to 363 K, carrying out hydrolysis with vigorous stirring (magnetic stirrer, rotation speed 450-500 rpm), introduction of a dopant in an amount of 0.15 mmol into the reaction mixture 1 minute after the start of NA hydrolysis and zeolite (0.3 g) – after 2 min (hydrolysis temperature T=368 K), separation of the obtained solid phase by vacuum filtration, washing with distilled water (20 ml, 3 times) and acetone (20 ml, 2 times) and drying at 363 K [65].

Nanocomposites NA/HZSM(12 40, 300) have been obtained by *Method 1a*, NA/HZSM(12, 25, 40, 300)-1 – by *Method 1b*, NA/HZSM(12, 25, 40)-2 – by *Method 2*, and NA:*M*/HZSM(40, 300)-3 with $M = V^{5+}$, Ni^{2+}, Ag^+ - by *Method 3*. Summary data on the studied objects are given in Table S2.

Table S2. Samples characterization methods [16, 33, 34, 54, 65, 66, 68, 69].

Sample	Method of obtaining	Characterization methods		
		Composition	Structure	Property
NA/HZSM(12) NA/HZSM(40) NA/HZSM(300)	1a	XRPD[1] (Section S2.1); FTIR spectroscopy (Section S2.2); BET[2] (Section S2.3); EDX[3] (Section S2.5); XPS[4] (Section S2.6)	XRPD[1] (Section S2.1); SEM[5] (Section S2.5)	PCA[6] (UV irradiation) with Si/Al=12 (Section S2.1.2.1); adsorption properties (Section S2.1.3); AMA[7] (Section S2.1.4)
NA/HZSM(12)-1 NA/HZSM(25)-1 NA/HZSM-5(40)-1	1b	XRPD[1] (Section S2.1); FTIR-spectroscopy (Section S2.2); BET[2] (Section S2.3); EDX[3] (Section S2.5); XPS[4] (Section S2.6); DSC[8] (Section S2.7); UV-VIS spectroscopy (Section S2.11); BJH[9] (Section S2.3);	XRPD[1] (Section S2.1); XAS[10] (Section S2.4); SEM[5] (Section S2.5)	CA[11] (propane conversion, ethanol conversion) (Sections S2.1.1.1, S2.2.2.2); PCA[6] (UV irradiation) (Section S2.1.2.1)

		MP-method (Section S2.3)		
NA/HZSM(12)-2 NA/HZSM(25)-2 NA/HZSM-5(40)-2	2	XRPD[1] (Section S2.1); FTIR-spectroscopy (Section S2.2); BET[2] (Section S2.3); EDX[3] (Section S2.5); XPS[4] (Section S2.6); DSC[8] (Section S2.7); UV-VIS spectroscopy (Section S2.11); BJH[9] (Section S2.3); MP-method (Section S2.3); TPD[12] (Section S2.10)	XRPD[1] (Section S2.1); XAS[10] (Section S2.4); SEM[5] (Section S2.5)	CA[11] (propane conversion, ethanol conversion) (Sections S2.1.1.1, S2.2.2.2); PCA[6] (UV irradiation) (Section S2.1.2.1)
NA:*M*/HZSM(40)-3 NA:*M*/HZSM(300)-3 *M*=V^{5+}, Ni^{2+}, Ag^{+}	3	XRPD[1] (Section S2.1); XPS[4] (Section S2.6); Chemiluminescence (Section S2.11)	XRPD[1] (Section S2.1); XAS[10] (Section S2.4); UV-DRS[13] (Section S2.8)	PCA[6] (visible light) (Section S2.1.2.2); adsorption properties (Section S2.1.3); AMA[7] (Section S2.1.4)
TS-1 TS-2 TS-3	-	XRPD[1] (Section S2.1); FTIR-spectroscopy (Section S2.2); BET[2] (Section S2.3); XPS[4] (Section S2.6); DSC[8] (Section S2.7); UV-VIS spectroscopy (Section S2.11); MP-method (Section S2.3); TPD[12] (Section S2.10)	XRPD[1] (Section S2.1); XAS[10] (Section S2.4)	CA[11] (propane conversion, ethanol conversion, allyl chloride conversion) (Sections S2.1.1.1, S2.1.1.2, S2.1.1.3)
TS-4	-	XRPD[1] (Section S2.1); FTIR-spectroscopy (Section S2.2); DSC[8] (Section S2.7); TPD[12] (Section S2.10)	XRPD[1] (Section S2.1); XAS[10] (Section S2.4)	CA[11] (allyl chloride conversion, propane conversion) (Sections S2.1.1.1, S2.1.1.3)

[1]XRPD - X-ray powder diffraction analysis; [2]BET - Brunauer–Emmett–Teller method; [3]EDX - Energy Dispersive X-Ray Spectroscopy; [4]XPS - X-ray Photoelectron Spectroscopy; [5]SEM - Scanning Electron Microscopy; [6]PCA - Photocatalytic Activity; [7]AMA - Antimicrobial Activity; [8]DSC - Differential Scanning Calorimetry; [9]BJH - Barrett–Joyner–Halenda method; [10]XAS - X-ray Absorption Spectroscopy; [11]CA - Catalytic Activity; [12]TPD - Temperature Programmed Desorption; [13]UV-DRS - UV-Vis diffuse reflectance spectroscopy

S2. Characterization Methods

Characterization methods were X-ray powder diffraction analysis (XRPD), FTIR spectroscopy, Brunauer–Emmett–Teller method (BET), Barrett–Joyner–Halenda method (BJH), MP-method, X-ray Absorption Spectroscopy (XAS), Scanning electron microscopy (SEM) with Energy Dispersive X-Ray Spectroscopy (EDX), X-ray photoelectron spectroscopy (XPS), Differential scanning calorimetry (DSC), UV-Vis diffuse reflectance spectroscopy (UV-DRS), Chemiluminescence Method, UV-VIS spectroscopy, Temperature Programmed Desorption (TPD), (Table S2).

S2.1. X-ray powder diffraction analysis (XRPD).

All the samples (HZSM(12, 25, 40, 300), NA/HZSM(12, 40, 300), NA/HZSM(12, 25, 40)-1, NA/HZSM(12, 25, 40)-2, NA:*M*/HZSM(40, 300)-3 (*M* = V^{5+}, Ni^{2+}, Ag^{+}), TS-1, TS-2, TS-3) have been studied using an HZG-4 diffractometer equipped with a flat graphite monochromator under CuK_α radiation (incremental mode) [16, 33, 54, 65]. X-ray powder diffraction study of HZSM(12, 25, 40), NA/HZSM(12, 25, 40)-1, NA/HZSM(12, 25, 40)-2, TS-1, TS-2, TS-3 was performed at X-ray structural analysis beamline of Kurchatov Synchrotron Radiation Source (λ = 0.78971 Å) [16, 33]. Phase analysis of the samples was qualitatively performed with the PCPDFWIN PDF-4+ database and data from [70]. A program [71] was used to process the diffractograms.

High-accuracy synchrotron measurements of HZSM(12, 40, 300) and NA/HZSM(12 40, 300), TS-4 samples were performed on the high-resolution powder diffraction beamline ID22 at the European Synchrotron Radiation Facility (ESRF, Grenoble, France) (λ = 0.399927(13) Å) [34]. The atomic structure and microstructure parameters of the studied samples were determined by Rietveld refinement using MRIA (HZSM (12, 40, 300), NA/HZSM (12, 40, 300) and TS-4) [72] and Jana2006 (TS-1, TS-2, TS-3) [73] programs. Diffraction profiles were modeled by the Voigt function [74] taking into account anisotropic line broadening [75].

S2.2. FTIR spectroscopy

FTIR spectra of HZSM(12, 25, 40, 300), NA/HZSM(12, 40, 300), NA/HZSM(12, 25, 40)-1, NA/HZSM(12, 25, 40)-2, TS-1, TS-2, TS-3, TS-4 were recorded on a Bruker EQUINOX 55 Fourier-transform infrared spectrometer with a 2 cm^{-1} resolution in the 400–4000 cm^{-1} frequency range in KBr pellets [16, 33, 34].

S2.3. Low temperature nitrogen adsorption method

The sorption capacities of HZSM(12, 25, 40, 300) and NA/HZSM(12, 40, 300) samples with reference to nitrogen were measured using the standard ASTM D4780-12 procedure by the Brunauer–Emmet–Teller (BET) method from a linear branch of the adsorption isotherm in the area of equilibrium relative pressures of nitrogen (0.05–0.30 P/P_0) [66]. Specific adsorption surface was determined from the t-diagram (dependence of the adsorbed gas volume on the adsorptive film thickness, t) [66].

The nitrogen adsorption measurements of HZSM(12, 25, 40), NA/HZSM(12, 25, 40)-1, NA/HZSM(12, 25, 40)-2, TS-1 and TS-2 were performed on an ASAP 2020-MP Micromeritics automatic high vacuum setup (United States) at 77 K in the range of relative pressures from 6.10 to 0.99. Specific adsorption surface was assessed by Brunauer–Emmett–Teller (BET) method; average pore hydraulic radius was evaluated by the micropore analysis method (MP method) [16, 33]. Pore volume of HZSM(12, 25, 40), NA/HZSM(12, 25, 40)-1, NA/HZSM(12, 25, 40)-2 was determined by the Barrett–Joyner–Halenda (BJH) method [33].

S2.4. X-ray Absorption Spectroscopy (XAS-method)

The XAS spectra (EXAFS and XANES) of NA/HZSM(12, 25, 40)-1, NA/HZSM(12, 25, 40)-2, NA:*M*/HZSM(40, 300)-3 (*M* = V^{5+}, Ni^{2+}, Ag^{+}), TS-1, TS-2, TS-3 and TS-4 at the K-edge of Ti were measured in fluorescence mode using an Amptek X123 silicon drift detector at the "Structural Materials Science" (STM) station of the Kurchatov synchrotron radiation source (Si (111) single-crystal monochromator, energy resolution ~ 1 eV) [16, 33, 65].

S2.5. Scanning electron microscopy (SEM) and energy-dispersive X-ray spectroscopy (EDS)

Scanning electron microscopy of HZSM(12, 25, 40, 300), NA/HZSM(12, 40, 300), NA/HZSM(12, 25, 40)-1, NA/HZSM(12, 25, 40)-2 was carried out using a JSM 7500F high-resolution electron microscope. [16, 66].

S2.6. X-ray photoelectron spectroscopy (XPS)

The surface composition of HZSM(12), NA/HZSM(12), NA:*M*/HZSM(40, 300)-3 (*M* = V^{5+}, Ni^{2+}, Ag^{+}) was studied via X-ray photoelectron spectroscopy (XPS) on a PHOIBOS 150 spectrometer equipped with a two- dimensional CCD detector (AlK_{α} radiation, ellipsoidal monochromator, and ΔE = 0.2 eV) and located at the Kurchatov synchrotron-neutron research complex [65, 67].

The surface composition of HZSM(12, 25, 40), NA/HZSM(12, 25, 40)-1, NA/HZSM(12, 25, 40)-2 was carried out on the complex photoelectron and raster Auger-electron spectrometer Thermo Fisher Scientific Escalab 250Xi ($AlK\alpha$ radiation, ultrahigh vacuum conditions with a base pressure no worse than 2×10^{-9} Torr) [16]

S2.7. Differential scanning calorimetry (DSC)

The thermal effects of HZSM(12, 25, 40), NA/HZSM(12, 25, 40)-1, NA/HZSM(12, 25, 40)-2, TS-1, TS-2, TS-3 and TS-4 under dynamic heating conditions were measured on a Netzsch DSC 204 Phoenix differential scanning calorimeter (99.99 % argon atmosphere, flow rate of 100 mL/min, temperature range of 213–873 K) [16, 33, 34].

S2.8. UV-Vis diffuse reflectance spectroscopy

UV-Vis diffuse reflectance spectra of semiconductor samples NA:*M*/HZSM(40, 300)-3 with *M* = V^{5+}, Ni^{2+}, Ag^{+} were presented on a Specord M40 spectrophotometer in the spectral range from 200 to 900 nm with a slit width of 2.5 to 20 nm [65].

S2.9. Chemiluminescence Method

Chemiluminescence spectra of NA:*M*/HZSM(40)-3 with *M* = V^{5+}, Ni^{2+}, Ag^{+} in the presence of luminol and lucigenin (under visible light irradiation) were recorded using a Lum-5773 chemiluminometer device [65]. The areas of the integrand curves (the values of *hv*, eV) correlating with the number of the Reactive Oxygen Species formed were calculated using a program [65].

S2.10. Temperature Programmed Desorption (TPD)

The acid sites concentration (C, μmol/g) of HZSM(12, 25, 40), NA/HZSM(12, 25, 40)-2 and TS-4 was studied by the method of temperature-programmed desorption of ammonia (TPD NH_3) (linear heating of 10 deg/min, constant helium supply rate of 1 cm^3/c, mass spectrometer as a detector) [16, 34].

S2.11. UV-VIS spectroscopy

Total acidity (N, mmol/g) of HZSM(12, 25, 40), NA/HZSM(12, 25, 40)-1, NA/HZSM(12, 25, 40)-2, TS-1, TS-2, TS-3 and TS-4 was studied by the adsorption of pyridine (Py) spectrophotometrically using a Specord spectrophotometer, UV-VIS (samples weighing of 10 mg, initial concentration of Py solution in octane was 0.3 μmol/L, solution volume of 5 mL) [16, 33, 34]. The equilibrium concentration substance was calculated by the formula:

$$N = (C_0 - C) \times \frac{V}{m} = (A_0 - A) \times \frac{V}{m} \times l \times E, \text{ [mol/g]}, \quad (1)$$

where A_0 and A are absorption coefficients of pyridine solution at the absorption maximum (λ_{max} = 252 nm), respectively, before and after the adsorption of pyridine, C_0 and C (μmol/L) are the concentration of the pyridine solution, respectively, before and after the adsorption of pyridine, m is the sample mass, V (mL) is the pyridine solution volume, l = 1 cm - cuvette thickness, $E = 2 \cdot 10^3$ L/mol·cm – the extinction [33, 34].

S2.12. Functional Properties

The samples were tested for catalytic (propane, ethanol and allyl chloride conversion), photocatalytic (decomposition of model organic dyes Methyl Orange and Rhodamine G under UV irradiation; triazole fungicide difenoxazole and pesticide thiamethoxam under visible light irradiation), adsorption (for the extraction of As(V), P(V), Se(VI) ions from aquatic media in the dark) and antimicrobial (against microorganisms *Staphylococcus aureus, Staphylococcus epidermidis, Escherichia coli, Bacillus anthracoides, Candida albicans* in the dark) properties.

S2.12.1. Catalytic properties

The catalytic activity of HZSM(Si/Al = 12, 25, 40), NA/HZSM(12, 25, 40)-1, NA/HZSM(12, 25, 40)-2, TS-1, TS-2 and TS-3 was studied in the reactions of propane (C_3H_8) (T = 298 - 1,143 K) and ethanol (C_2H_5OH) (T = 413 – 653 K) conversion [16, 33, 34]. The catalytic activity of TS-1, TS-2, TS-3 and TS-4 was studied in the reaction of allyl chloride conversion (T= 303 K) [33, 34].

S2.12.1.1. Propane conversion

Measurements were taken using a flow-through unit with a U-shaped quartz reactor according to the method decscribed in [16, 33]. High-purity propane (99.98 wt.%) was used as a raw material, the flow rate was 1.25 mL/s, and the contact time with the catalyst was 0.6 seconds. The experimental data presented in the work is an average value obtained from three consecutive analyzes of propane dehydrogenation products. The holding time between products analysis was 40 minutes to achieve a steady state.

The propane conversion was determined by the amount of propane reacted:

$$\alpha = \frac{n_{init} - n_{res}}{n_{init}}, [\%], \quad (2)$$

where n_{init} and n_{res} are respectively, the initial and residual molar amount of propane. The calculation of the main components release rate (value w) was carried out according to the equation:

$$W = \frac{K \times W_{ex} \times S}{V_{loop}}, [\mu M/(g \times s)], \quad (3)$$

where K is a correction factor: 1.1×10^{-5} μM/mV × s, W_{ex} - reaction mixture exit rate, s - chromatographic peak area, V_{loop} – sampling loop volume.

Selectivity for each component was calculated by the formula:

$$S_i = \frac{a_i \times n_{i_{ex}}}{n_{C3H8_{entr}} - n_{C3H8_{ex}}}, [\%] \quad (4)$$

where a_i, - a number of carbon atoms in the product (i), $n_{i_{ex}}$ – a molar flow of product (i) at the output from the reactor, $n_{C3H8_{entr}}$ and $n_{C3H8_{ex}}$ – a molar flux of C_3H_8, respectively, at the input and output from the reactor.

TON value (turnover number) is the "number of revolutions", defined as the number of moles of the product (M_i: i=C_3H_6 or C_2H_4), formed on one moles of catalyst (M_{kat}) until (t-process duration) the catalyst has completely lost its activity:

$$TON = \frac{M_i}{M_{kat}} = TOF_{sur} \times t, \quad (5)$$

where TOF_{sur} is the maximum number of molecules (moles) of the product formed per unit time at one active site (actually, at one molecule, one mole) of the catalyst. TON was calculated taking into account the change in catalytic sites in the row: 75.6 μmol/g (HZSM-5(40)), 112.8 μmol/g (HZSM-5(25)), 169.9 μmol/g (HZSM-5(12)) presented in works [76].

The activation energies of the process were calculated for all the catalysts studied:

$$\ln w = \ln A - \frac{E_a}{RT}, \; E_a \text{ [kJ/mol]} \quad (6)$$

where A is the Arrhenius constant (can be found experimentally by the shift of the function graph along the ordinate), R is the universal gas constant (8.314 J/(mol·K)), Ea, kJ/mol - activation energy of propane cracking process.

S2.12.1.2. Ethanol dehydration/dehydrogenation

Measurements were carried out in a flow quartz reactor with a fixed layer. Before the experiment, the catalysts were subjected to the standard thermal treatment in a helium flow at 673 K for 1 h [16, 33]. A gas chromatograph Chromatech Crystal 5000 was used to test the catalytic properties, separation on a column packed with Porapak Q at 408 K, FID detector. The ethanol conversion, products selectivity and yield are defined by equations 2 - 4.

S2.12.1.3. Allyl chloride conversion

Measurements were carried out at T = 303 K in the closed batch reactor and the isothermal mode with intensive stirring (reaction time of 85 and 120 min) [33, 34]. The reaction mixture composition was analyzed by gas chromatography using an internal standard (glass packing column 3 m long, 3 mm in diameter, chromatographic phase 3 % OV17 deposited on chromaton-N-super, helium as the carrier gas) [33, 36]. The hydrogen peroxide concentration was determined by iodometric titration.

S2.12.2. Photocatalytic activity (PCA)

Photocatalytic activity (PCA) in an aqueous medium was studied in photodegradation reaction of methyl orange (MeO; $C_{14}H_{14}N_3O_3SNa$, CAS no. 547-58-0) on NA/HZSM(12, 40, 300), NA/HZSM(12, 25, 40)-1, NA/HZSM(12, 25, 40)-2 samples and Rhodamine 6G (R6G; $C_{28}H_{31}ClN_2O_3$, CAS no. 989-38-8) on HZSM(12) under UV irradiation, as well as real pollutants triazole fungicide difenoconazole and pesticide thiamethoxam on NA:M/HZSM(40, 300)-3, M = V^{5+}, Ni^{2+}, Ag^{+} samples under visible light irradiation at $\lambda >$ 450 nm [54, 65, 66].

S2.12.2.1. Photodegradation reaction of model dyes (UV irradiation)

A powdered sample (the weight content in dye solution was 0.05 g/L) were added to the aqueous dye (MeO or R6G) solution (initial concentration of 0.05mmol/L, pH ~ 3–4). The resulting suspension (50 mL) was irradiated with UV light (250 – 400 nm, Camelion UV lamp, 26 W) in an open container at constant stirring for 240 min. The solid phase was separated by centrifugation (OPn-8UKhL42 centrifuge).

The used photoreaction model refers to reactions of a pseudo first order, for which the rate constant (k) was calculated as the slope of the dependence of the change in the substrate concentration (c/c_0) on the irradiation time τ in rectifying semilogarithmic coordinates [54].

S2.12.2.2. Photodegradation reaction of real pollutants (visible light)

The photocatalytic activity was studied under visible light irradiation (a luminescent lamp, Camelion 45 W, λ = 450 nm). Initial concentrations of triazole fungicide difenoxazole and pesticide thiamethoxam were 0.06 mmol/L and 0.05 mmol/L correspondingly. The concentration of organic contaminants in water was measured once every 30 min using an Akvilon SF200 spectrophotometer [65].

S2.12.3. Adsorption properties in the dark

Adsorption capacity was studied using model aqueous solutions containing P(V) (H_3PO_4) (samples: HZSM(12, 40, 300), NA/HZSM(12, 40, 300), NA:*M*/HZSM(40, 300)-3, *M* = V^{5+}, Ni^{2+}, Ag^{+}), As(V) (H_3AsO_4) and Se(VI) (H_2SeO_4) (samples: NA:*M*/HZSM(40, 300)-3, *M* = V^{5+}, Ni^{2+}, Ag^{+}) at a concentration of 10 mg/L. The concentrations of the elements in the final solutions after adsorption (C_{final}) as well as the initial concentration of the elements (C_{init}) were measured by inductively coupled plasma atomic emission spectrometry (ICPE-spectrometry, ICPE-9000 Shimadzu, Japan). The degree of adsorption of elements (R, %) was calculated using the formula:

$$R = 100 \times \left[1 - \frac{c_{final}}{c_{init}}\right], \quad (7)$$

The standard deviation was 2 % [54, 65, 66].

S2.12.4. Antimicrobial activity in the dark (AMA)

Antimicrobial properties against *Staphylococcus epidermidis, Escherichia coli, Bacillus anthracoides* were studied on HZSM(12, 40, 300), NA/HZSM(12, 40, 300), NA:*M*/HZSM(40, 300)-3 (*M* = V^{5+}, Ni^{2+}, Ag^{+}) samples as well as against *Staphylococcus aureus* and *Candida albicans* on HZSM(12, 40, 300) and NA/HZSM(12, 40, 300) samples in accordance with the methodological guidelines MUK 4.2.1890-04 (Determination of the sensitivity of microorganisms to antibiotics). Microbiological studies were performed in a box irradiated with an UV lamp for sterilization prior to seeding the test cultures on growth media. The degree of microorganisms sensitivity to the test samples was estimated from the size of the zone of no microorganism growth. [54, 65].

Table S3. Some characteristics of HZSM and NA/HZSM (Data from [16, 66]).

Sample	Si/Al	Textural characteristics							Particle or associate size: N, nm (SEM)		Elements, wt. % (EDX)				
		V_{μ}[1], cm^3/g	V_{meso}, cm^3/g	S_{BET}[2], m^2/g	S_{ext}[3], m^2/g	Surface energy[4], KJ/cm^3	Particle size[5], nm	r_p[6], nm	Faceted	Spherical	Si	Al	O	Ti	S
HZSM(12)	12	0.139	0.129*/0.135**	299	20-33	0.29	20.0	0.260	~120-600	≤215 N_{min}~20	-[7]	-[7]	-[7]	-[7]	-[7]
NA/HZSM(12)	-[7]	-[7]	-[7]	322	131.9	-[7]	-[7]	-[7]	-	≤300; N_{min}~20	10.51	0.73	39.32	12.92	1.31
NA/HZSM(12)-1	-[7]	0.119	0.120*/0.122**	249	-[7]	0.19	20.7	0.140	-	≤300; N_{min}~20	12.61	0.78	47.71	12.07	1.28
NA/HZSM(12)-2	-[7]	0.102	0.100*/0.117**	148	-[7]	0.29	20.9	0.210	~120-4800	≤350; N_{min}~20	4.54	0.42	40.18	54.77	0.09
HZSM(25)	25	0.143	0.156*/0.160**	319	29	0.29	19.0	0.310	~480-4600	≤250; N_{min}~20	44.34	2.79	52.86	-	-
NA/HZSM(25)-1	-[7]	0.113	0.111*/0.101**	257	-[7]	0.38	30.0	0.290	~480-4600	≤250; N_{min}~20	20.38	1.15	39.60	24.11	1.85
NA/HZSM(25)-2	-[7]	0.071	0.173*/0.175**	167	-[7]	0.47	35.8	0.220	~480-2000	≤410; N_{min}~20	15.26	1.14	37.22	46.37	0.01
HZSM(40)	40	0.076	0.185*/0.192**	353	68	-[7]	-[7]	-[7]	-	~ 600; N_{min}~20	-[7]	-[7]	-[7]	-[7]	-[7]
NA/HZSM(40)	-[7]	-[7]	-[7]	312	72.9	0.11	19.9	0.298	-	~300-2000; N_{min}~25	33.67	-	60.9	5.72	1.15
NA/HZSM(40)-1	-[7]	0.145	0.115*/0.120**	264	-[7]	0.16	27.9	0.272	-	≤590; N_{min}~25	36.51	1.08	57.26	4.99	0.16
NA/HZSM(40)-2	-[7]	0.142	0.102*/0.107**	170	-[7]	0.13	35.0	0.357	-	≤300; N_{min}~60	16.27	0.34	30.25	53.14	-
HZSM(300)	300	-[7]	-[7]	414	-[7]	-[7]	-[7]	-[7]	~220-2000	≤250; N_{min}~20	-[7]	-[7]	-[7]	-[7]	-[7]
NA/HZSM(300)	-[7]	-[7]	-[7]	293	182.7	-[7]	-[7]	-[7]	-	≤720; N_{min}~20	23.83	-	33.01	11.85	1.57

[*] mesopore volume calculated from the adsorption branch by BJH method; [**]mesopore volume calculated from the desorption branch by BJH method; [1] microporous space volume; [2] total surface (BET); [3] external surface; [4] the surface energy of adsorption centers, determined by the Temkin equation; [5] the average particle size of powders (nm) calculated by the formula $N = A/(S_{BET} \times \varrho)$ (A is an empirical value, including pore volume, width, area and fraction of pores in the sample, ϱ is the density of the material, g/m^3) using BET method data and software ASAP 20020 plus, Micromeritics (USA); [6] average pore hydraulic radius defined using MP method and software ASAP 20020 plus, Micromeritics (USA); [7] measurements were not made

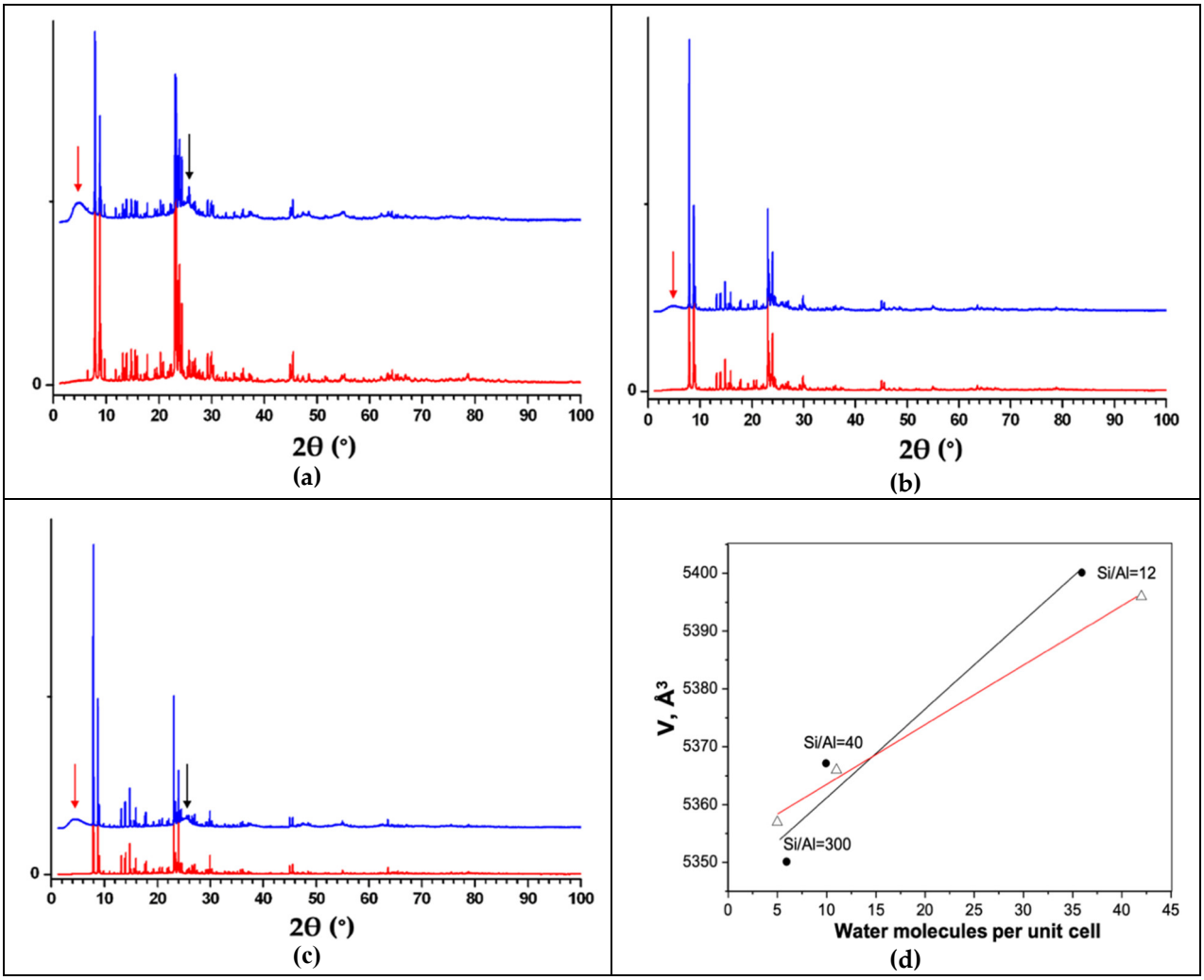


Figure S1. Diffraction patterns of HZSM (red), NA/HZSM (*Method 1a*) (blue): Si/Al = 12 **(a)**, 40 **(b)**, 300 **(c)** (λ –1.54051 Å) and the relationship between HZSM (•) and NA/HZSM (△) unit cell volume and water molecules content in the framework cavities (XRPD) **(d)**. Red arrow marks silicon-containing oxygenous formations, black arrow - nanoscale anatase.

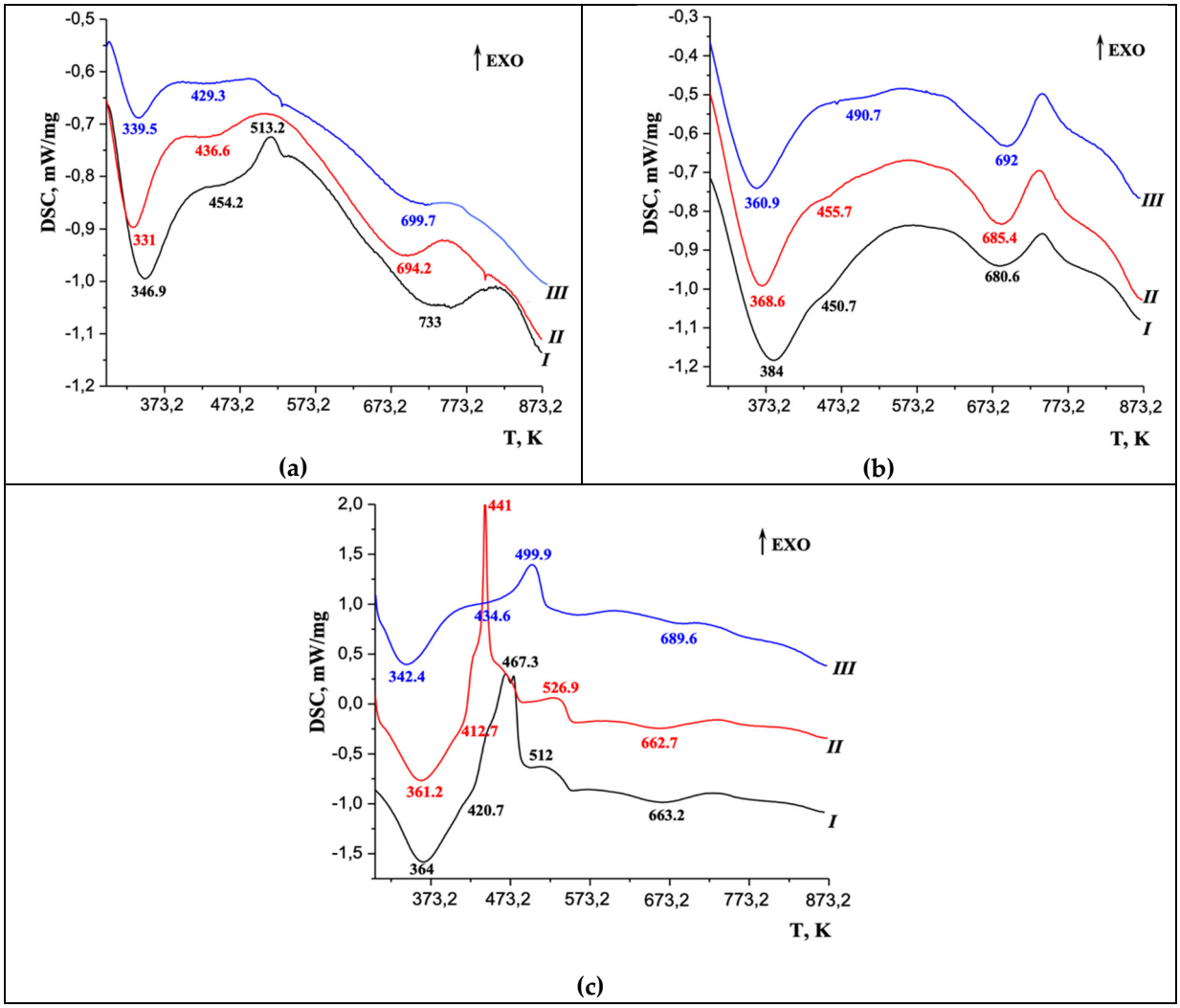


Figure S2. DSC thermograms of HZSM zeolites **(a)** and NA/HZSM nanocomposites obtained by *Method 1b* - NA/HZSM-1 **(b)** and *Method 2* - NA/HZSM-2 **(c)**: *I* – Si/Al=12, *II* – Si/Al=25, *III* – Si/Al=40.

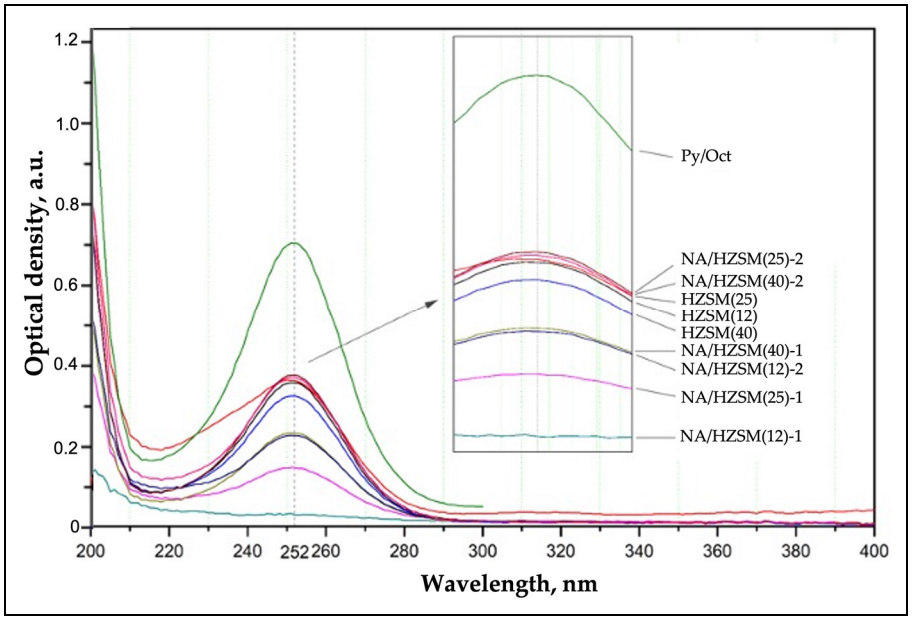


Figure S3. UV-Vis spectra of pyridine adsorption on HZSM, NA/HZSM-1 and NA/HZSM-2

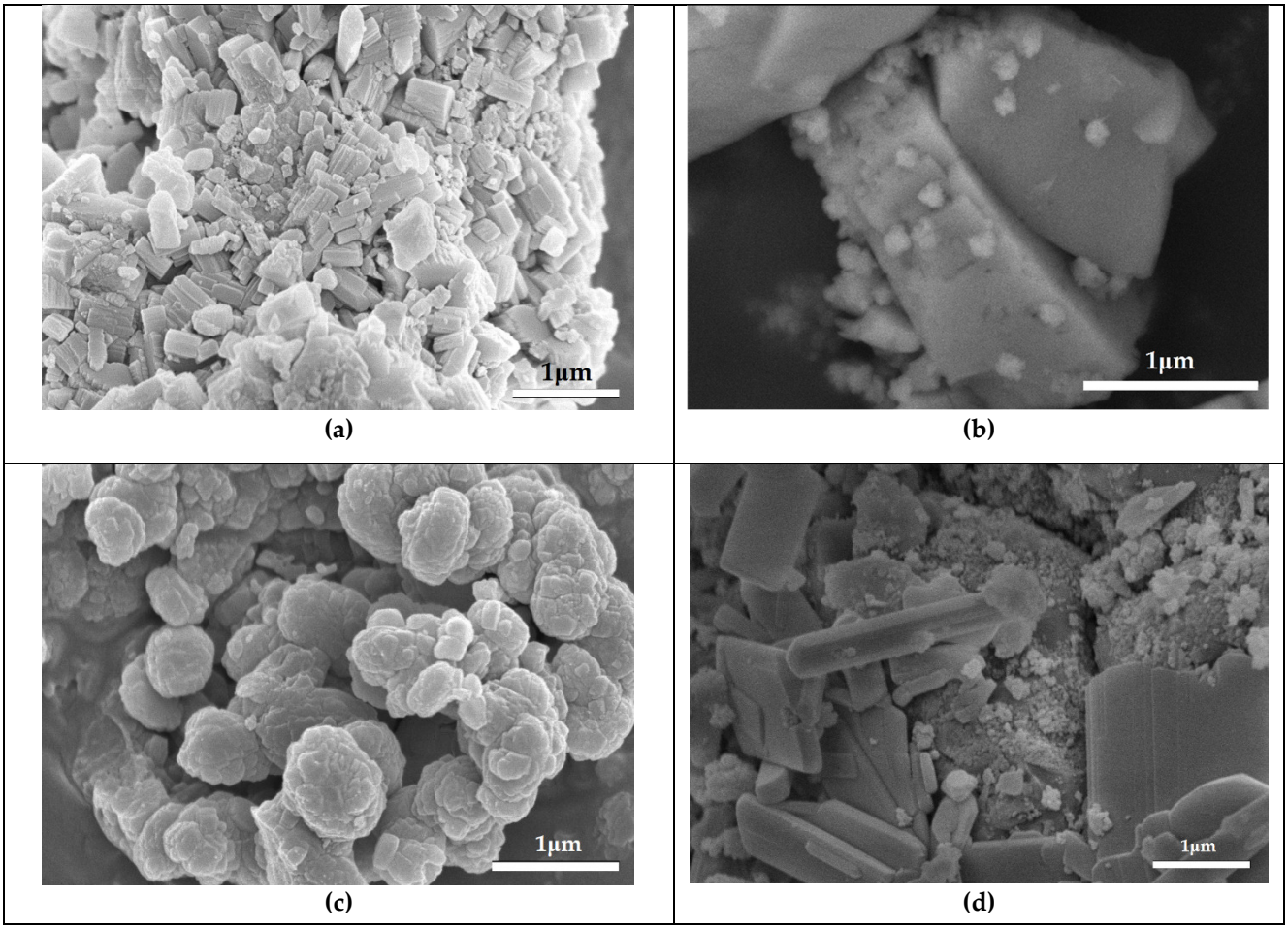


Figure S4. SEM images of HZSM(12) (a), HZSM(25) (b), HZSM(40)(c), HZSM(300)(d)

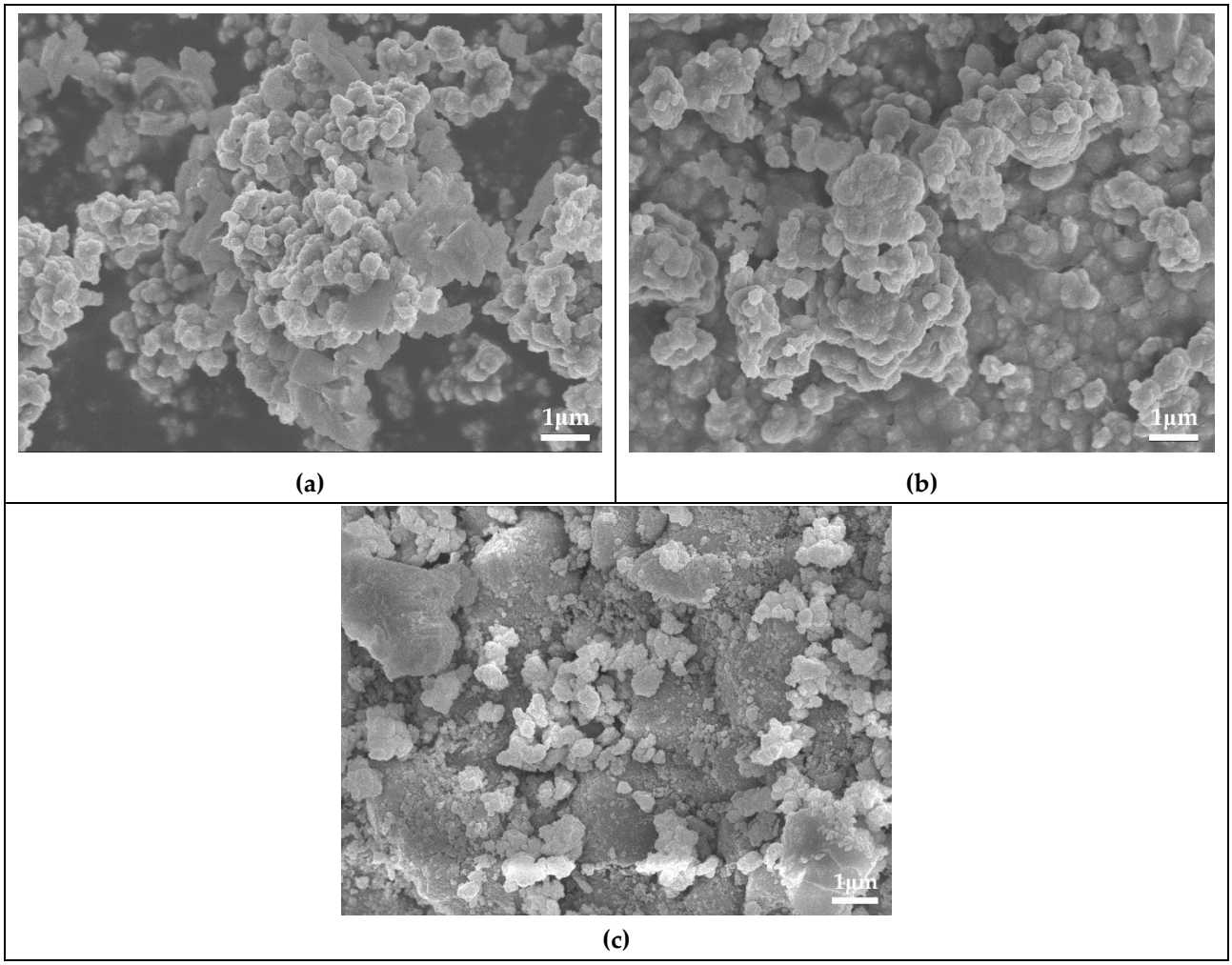


Figure S5. SEM images of NA/HZSM(12) (a), NA/HZSM(40) (b), NA/HZSM(300) (c)

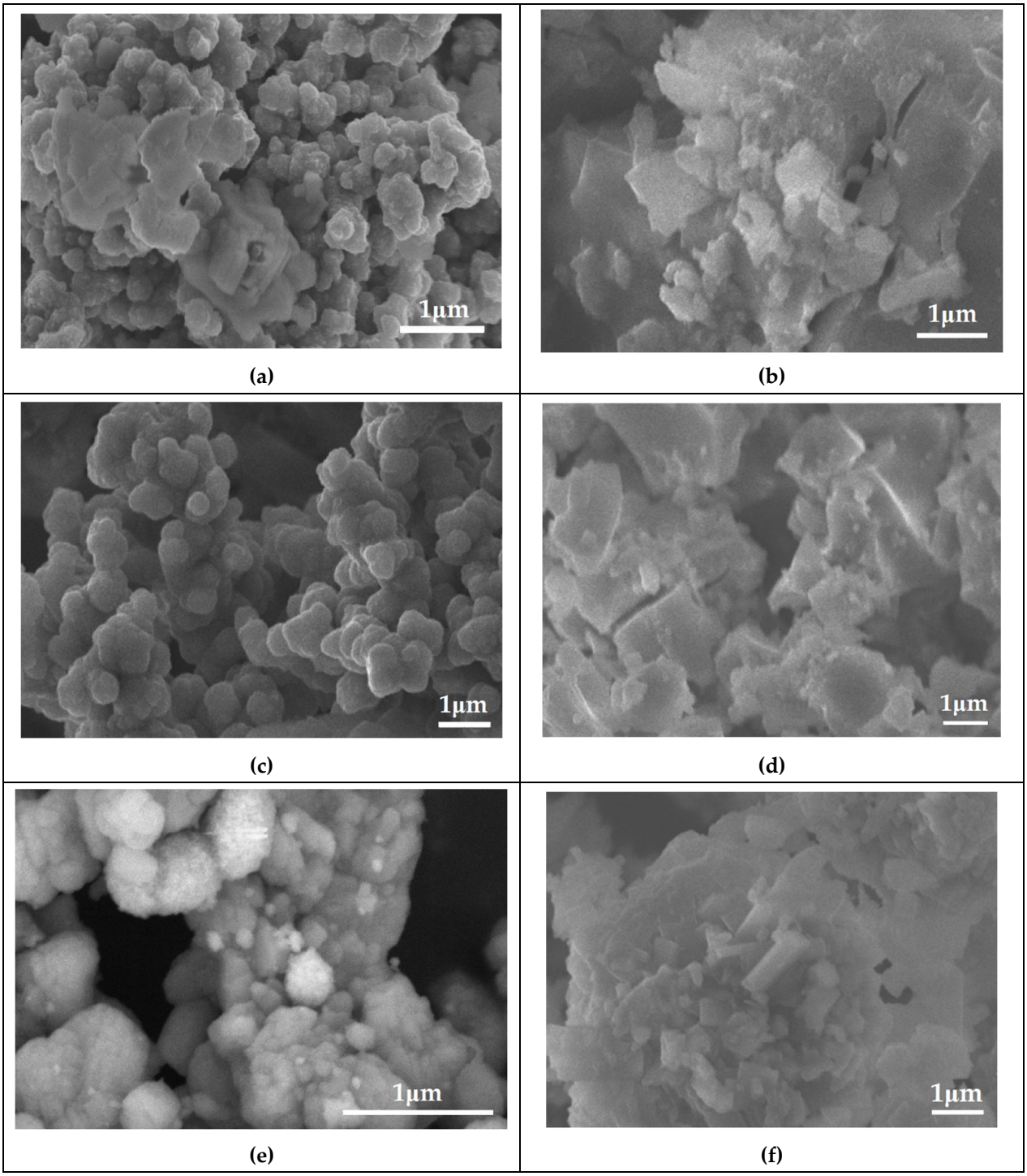
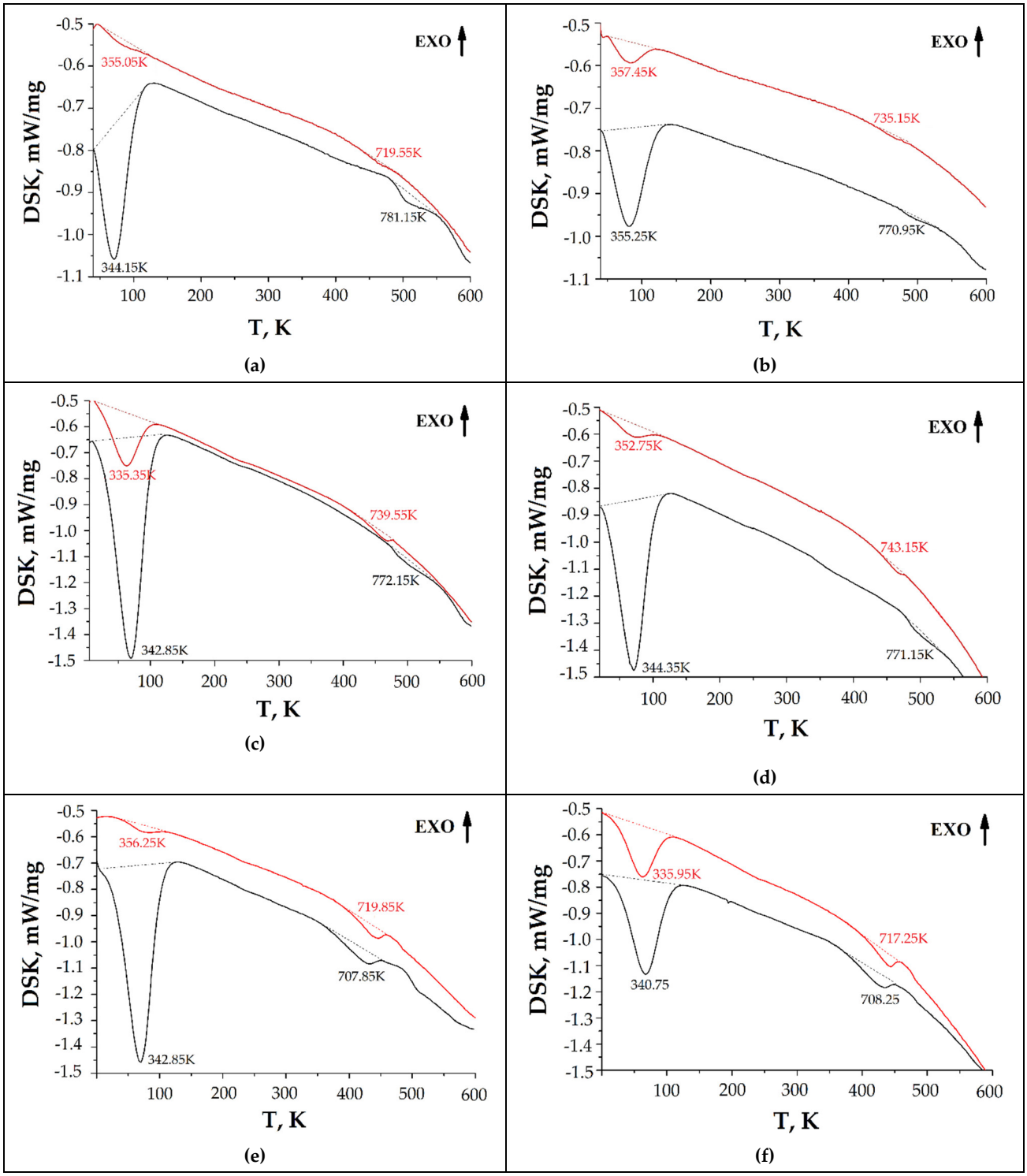


Figure S6. SEM images of NA/HZSM(12)-1 (a), NA/HZSM(12)-2 (b), NA/HZSM(40)-1 (c), NA/HZSM(40)-2 (d), NA/HZSM(300)-1(e), NA/HZSM(300)-2(f).


EXO
DSK, mW/mg
T, K
355.05K
719.55K
781.15K
344.15K
(a)
EXO
DSK, mW/mg
T, K
357.45K
735.15K
355.25K
770.95K
(b)
EXO
DSK, mW/mg
T, K
335.35K
739.55K
772.15K
342.85K
(c)
EXO
DSK, mW/mg
T, K
352.75K
743.15K
344.35K
771.15K
(d)
EXO
DSK, mW/mg
T, K
356.25K
719.85K
707.85K
342.85K
(e)
EXO
DSK, mW/mg
T, K
335.95K
717.25K
340.75
708.25
(f)

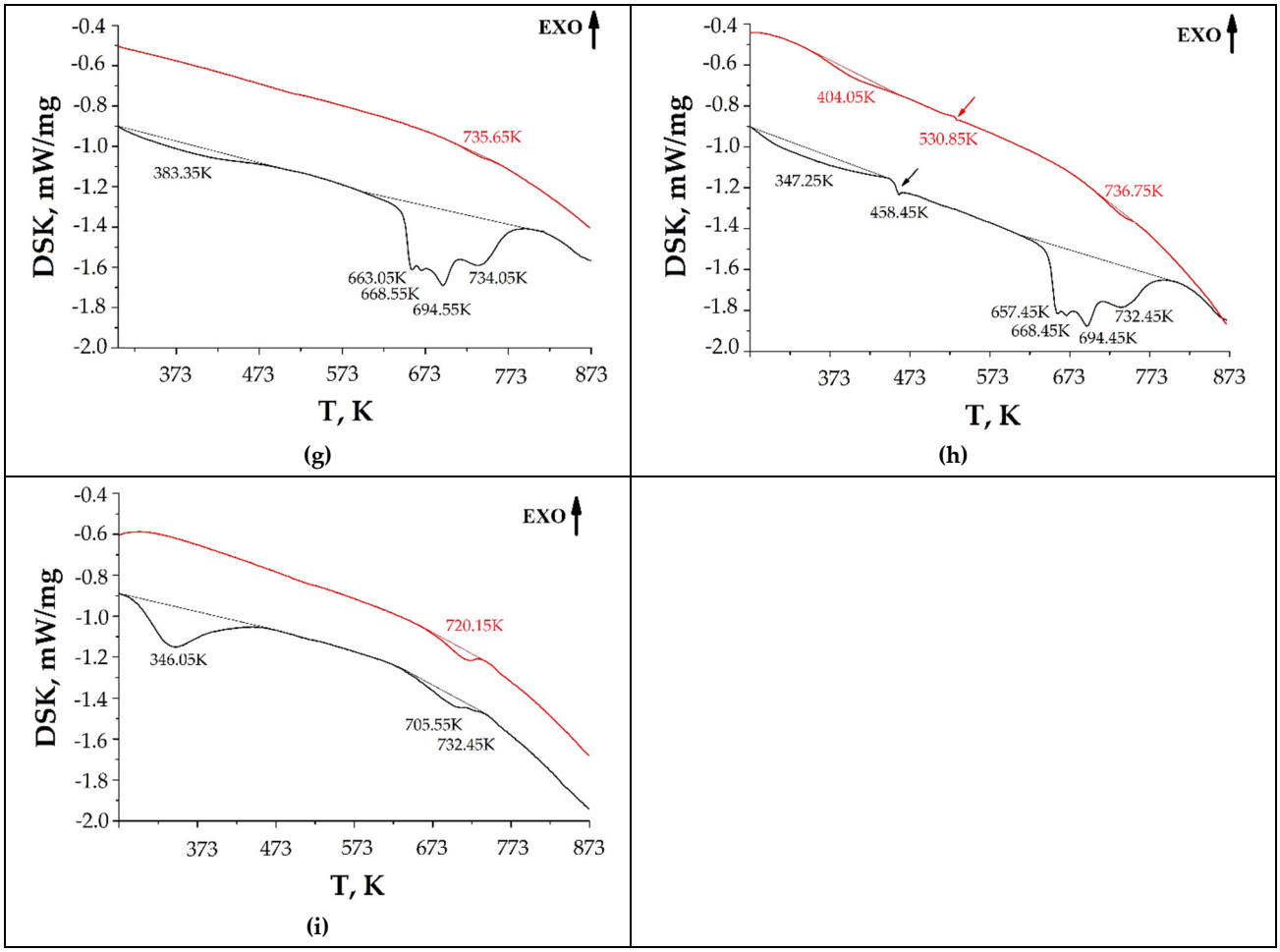


Figure S7. DSC thermograms of TS-1 (a), TS-1(348) (b), TS-2 (c), TS-2(348) (d), TS-3(e), TS-3(348) (f), TS-4(g), TS-4(348) (h) and TS-4(348) (i) recorded into two stages: first scanning is a black line, and second scanning (after sample cooling to the initial experimental temperature) is a red line